The implementation of the scheme requires flux linkages and torque c(tations, plus generation of switching states through a feedback control of the t and flux directly without inner current loops.

The stator q and d axes flux linkages are

$$\lambda_{qs} = \int(v_{qs} - R_s i_{qs})\,dt \qquad (8.19)$$
$$\lambda_{ds} = \int(v_{ds} - R_s i_{ds})\,dt \qquad (8.20)$$

where the direct and quadrature axis components are obtained from the *abc* ables by using the transformation,

$$i_{qs} = i_{as} \qquad 8.21$$
$$i_{ds} = \frac{1}{\sqrt{3}}(i_{cs} - i_{bs}) \qquad 8.22$$

This transformation is applicable for voltages and flux linkages as well. To o uniformly rotating stator flux, note that the motor voltages have to be variec formly without steps too. This imposes a requirement of continuously variabl tor voltages with infinite steps, which is not usually met by the inverter beca has only finite switching states.

Switching States of the Inverter Consider the inverter shown in Figure 8.8. The terminal voltage a with respect to negative of the dc supply is considered, and Va is determined by a set of switches, S_a, consisting of T_1 and T_4 as shown in the Table 8.1. When the switching devices T_1 and T_4 and their antiparallel diodes are off, indeterminate. Such a situation is not encountered in practice and, hence, has not been considered. The switching of S_b and S_c sets for line b and c can be similarly derived. The total number of switching states possible with S_a, S_b, and S_c is eight; they are elaborated in Table 8.2 by using the following relationships:

$$\left.\begin{aligned} v_{ab} &= v_a - v_b \\ v_{bc} &= v_b - v_c \\ v_{ca} &= v_c - v_a \end{aligned}\right\} \qquad (8.23)$$

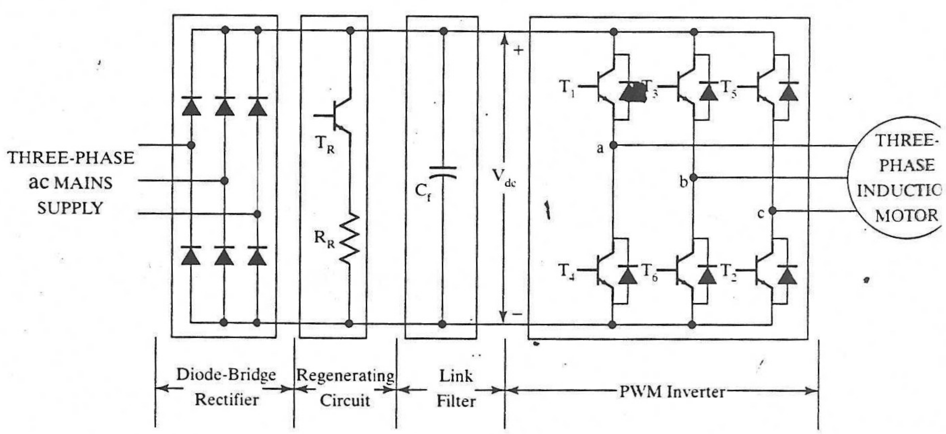

Figure 8.8 Power-circuit configuration of the induction motor drive

TABLE 8.1 Switching states of inverter phase leg *a*

T_1	T_4	S_a	V_a
on	off	1	V_{dc}
off	on	0	0

TABLE 8.2 Inverter switching states and machine voltages

States	S_a	S_b	S_c	V_a	V_b	V_c	V_{ab}	V_{bc}	V_{ca}	V_{as}	V_{bs}	V_{cs}	V_{qs}	V_{ds}
I	1	0	0	V_{dc}	0	0	V_{dc}	0	$-V_{dc}$	$\frac{2}{3}V_{dc}$	$-\frac{1}{3}V_{dc}$	$-\frac{1}{3}V_{dc}$	$\frac{2}{3}V_{dc}$	0
II	1	0	1	V_{dc}	0	V_{dc}	V_{dc}	$-V_{dc}$	0	$\frac{1}{3}V_{dc}$	$-\frac{2}{3}V_{dc}$	$\frac{1}{3}V_{dc}$	$\frac{1}{3}V_{dc}$	$\frac{V_{dc}}{\sqrt{3}}$
III	0	0	1	0	0	V_{dc}	0	$-V_{dc}$	V_{dc}	$-\frac{1}{3}V_{dc}$	$-\frac{1}{3}V_{dc}$	$\frac{2}{3}V_{dc}$	$-\frac{1}{3}V_{dc}$	$\frac{V_{dc}}{\sqrt{3}}$
IV	0	1	1	0	V_{dc}	V_{dc}	$-V_{dc}$	0	V_{dc}	$-\frac{2}{3}V_{dc}$	$\frac{1}{3}V_{dc}$	$\frac{1}{3}V_{dc}$	$-\frac{2}{3}V_{dc}$	0
V	0	1	0	0	V_{dc}	0	$-V_{dc}$	V_{dc}	0	$-\frac{1}{3}V_{dc}$	$\frac{2}{3}V_{dc}$	$-\frac{1}{3}V_{dc}$	$-\frac{1}{3}V_{dc}$	$-\frac{V_{dc}}{\sqrt{3}}$
VI	1	1	0	V_{dc}	V_{dc}	0	0	V_{dc}	$-V_{dc}$	$\frac{1}{3}V_{dc}$	$\frac{1}{3}V_{dc}$	$-\frac{2}{3}V_{dc}$	$\frac{1}{3}V_{dc}$	$-\frac{V_{dc}}{\sqrt{3}}$
VII	0	0	0	0	0	0	0	0	0	0	0	0	0	0
VIII	1	1	1	V_{dc}	V_{dc}	V_{dc}	0	0	0	0	0	0	0	0

and machine phase voltages for a balanced system are

$$\left.\begin{aligned} v_{as} &= \frac{(v_{ab} - v_{ca})}{3} \\ v_{bs} &= \frac{(v_{bc} - v_{ab})}{3} \\ v_{cs} &= \frac{(v_{ca} - v_{bc})}{3} \end{aligned}\right\} \tag{8.24}$$

and q and d axes voltages are given by

$$\left.\begin{aligned} v_{qs} &= v_{as} \\ v_{ds} &= \frac{1}{\sqrt{3}}(v_{cs} - v_{bs}) = \frac{1}{\sqrt{3}} v_{cb} \end{aligned}\right\} \tag{8.25}$$

The stator q and d voltages for each state are shown in Figure 8.9. The limited states of the inverter create distinct discrete movement of the stator-voltage phasor, v_s consisting of the resultant of v_{qs} and v_{ds}. An almost continuous and uniform flux phasor is feasible with these discrete voltage states, one due to their integration over time as seen from equations (8.19) and (8.20).

For control of the voltage phasor both in its magnitude and phase, the requested voltage vector's phase and magnitude are sampled, say once every

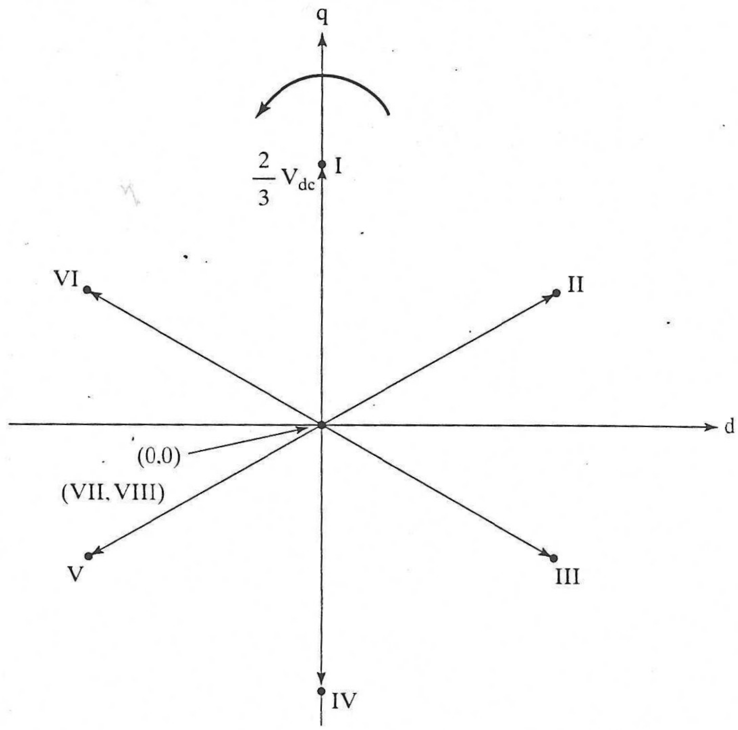

Figure 8.9 The inverter output voltages corresponding to switching states

switching period. The phase of the requested voltage vector identifies the nearest two nonzero voltage vectors. The requested voltage vector can be synthesized by using fractions of the two nearest voltage vectors, which amounts to applying these two vectors, one at a time, for a fraction of the switching period. The nearest zero voltage vector to the two voltage vectors is applied for the remaining switching period. The duty cycle for each of the voltage vectors is determined by the phasor projection of the requested voltage vector onto the two nearest voltage vectors. This method of controlling the input voltages to the machine through a synthesis of voltage phasor rather than the individual line-to-line voltages has the advantages of: (i) not using pulse-width modulation carrier-frequency signals, (ii) higher fundamental voltages compared to sine-triangle PWM, based controllers, (iii) given the switching frequency, the switching losses are minimized, and (iv) lower voltage and current ripples. This method of switching the inverter is known as space vector modulation (SVM) and many variations are available in literature.

Flux control A uniform rotating stator flux is desirable, and it occupies one of the sextants (in the phasor diagram shown in Figure 8.10) at any time. The stator-flux phasor has a magnitude of λ_s, with an instantaneous position of θ_{fs}. The corresponding d and q axes components are λ_{ds} and λ_{qs}, respectively. Assuming that a feedback of stator flux is available, its place in the sextant is identified from its position. Then the influencing voltage phasor is identified by giving a 90° phase shift. For example, if the stator-flux phasor is in sextant <2>, the right influencing

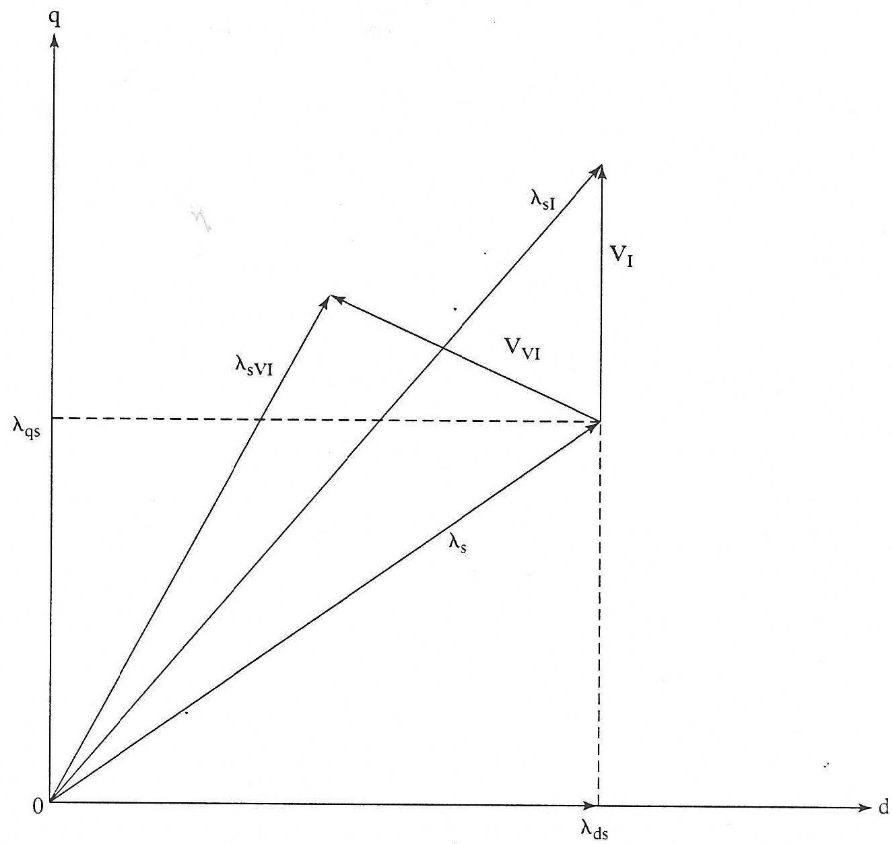

Figure 8.11 Effect of switching v_I and v_{VI} on stator-flux phasor

The error torque is processed through a window comparator to produce digital outputs, S_T, as follows:

Condition	S_T
$(T_e^* - T_e) > \delta T_e$	1
$-\delta T_e < (T_e^* - T_e) < \delta T_e$	0
$(T_e^* - T_e) < -\delta T_e$	−1

where δT_e is the torque window acceptable over the commanded torque. When the error exceeds δT_e, it is time to increase the torque, denoting it with a +1 signal. If the torque error is between positive and negative torque windows, then the voltage phasor could be at zero state. If the torque error is below $-\delta T_e$, it amounts to calling for regeneration, signified by −1 logic signal.

Interpretation of S_T is as follows: when it is 1 amounts to increasing the voltage phasor, 0 means to keep it at zero, −1 requires retarding the voltage phasor behind the flux phasor to provide regeneration. Combining the flux error output S_λ, the torque error output S_T, and the sextant of the flux phasor S_θ, a switching table can be realized to obtain the switching states of the inverter; it is given in Table 8.3. The algorithm for S_θ is shown in Table 8.4.

TABLE 8.3 Switching states for possible S_λ, S_T, and S_θ

		S_θ					
S_λ	S_T	<1>	<2>	<3>	<4>	<5>	<6>
1	1	VI (1,1,0)	I (1,0,0)	II (1,0,1)	III (0,0,1)	IV (0,1,1)	V (0,1,0)
1	0	VIII (1,1,1)	VII (0,0,0)	VIII (1,1,1)	VII (0,0,0)	VIII (1,1,1)	VII (0,0,0)
1	−1	II (1,0,1)	III (0,0,1)	IV (0,1,1)	V (0,1,0)	VI (1,1,0)	I (1,0,0)
0	1	V (0,1,0)	VI (1,1,0)	I (1,0,0)	II (1,0,1)	III (0,0,1)	IV (0,1,1)
0	0	VII (0,0,0)	VIII (1,1,1)	VII (0,0,0)	VIII (1,1,1)	VII (0,0,0)	VIII (1,1,1)
0	−1	III (0,0,1)	IV (0,1,1)	V (0,1,0)	VI (1,1,0)	I (1,0,0)	II (1,0,1)

TABLE 8.4 Flux-phasor sextant logic (S_θ)

θ_{fs}	Sextant
$0 \leq \theta_{fs} \leq \pi/3$	<2>
$-\pi/3 \leq \theta_{fs} \leq 0$	<3>
$-2\pi/3 \leq \theta_{fs} \leq -\pi/3$	<4>
$-\pi \leq \theta_{fs} \leq -2\pi/3$	<5>
$2\pi/3 \leq \theta_{fs} \leq \pi$	<6>
$\pi/3 \leq \theta_{fs} \leq 2\pi/3$	<1>

Consider the first column corresponding to S_θ = <1>. The switching states of the inverter are indicated in parentheses; they correspond to S_a, S_b, and S_c. The flux error signal indicates 1, which means the flux is less than its request value and therefore the flux phasor has to be increased. At the same time, torque error is positive, asking for an increase. Merging these two with the position of the flux phasor in <1>, the voltage phasor I and VI satisfy the requirements only if the flux is within the first 30° of the sextant <1>. In the second 30°, note that the voltage phasor I will increase the flux-phasor magnitude but will retard it in phase. This will result in a reduction of the stator frequency and reversal of the direction of torque. The control requires the advancement of the flux phasor in the same direction (i.e., counterclockwise in this discussion); that could be satisfied only by voltage phasor VI in this 30°. Voltage phasor VI is the only one satisfying the uniform requirements throughout the sextant <1>, so the voltage phasor VI is chosen for S_T and S_λ to be equal to +1 with the flux phasor in sextant <1>. When the torque error is zero, the only logical choice is to apply zero line voltages; because the previous state had two +1 states, it is easy to achieve zero line voltages by choosing the switching state VIII with all ones. If the torque error becomes negative with $S_T = -1$, the machine has to regenerate, with a simultaneous increase in flux phasor due to $S_\lambda = 1$; hence, the voltage phasor is retarded close to the flux phasor, and, hence, switching state II(1, 0, 1) is selected.

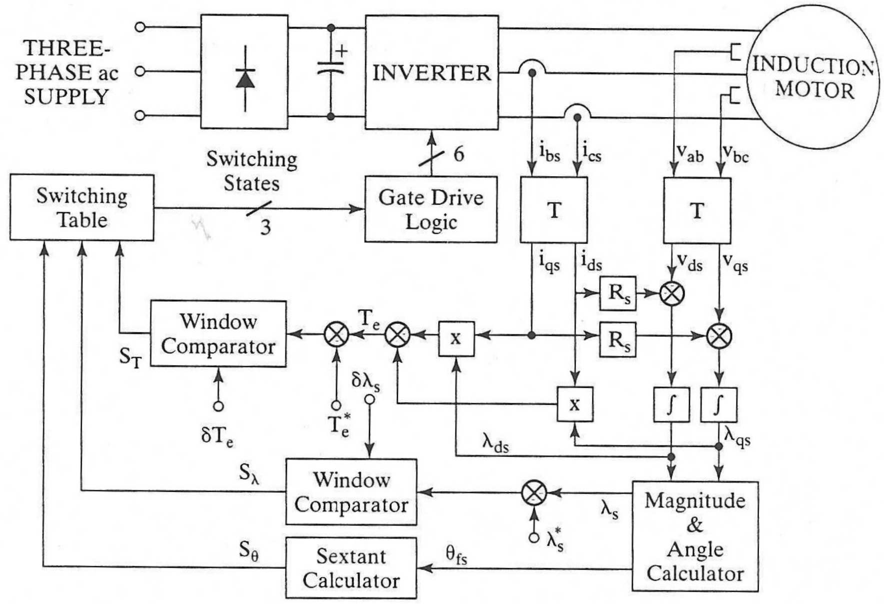

Figure 8.12 Block-diagram schematic of the direct torque (self) induction motor drive

If $S_\lambda = 0$ (i.e., the flux phasor has exceeded its request by the hysteresis window amount, $\delta\lambda_s$), then it has to be decreased to match its request value by choosing a voltage phasor away from flux phasor, i.e., V. This accelerates the flux phasor and increases the slip speed, resulting also in an increase of electromagnetic torque, thus satisfying $S_T = 1$ demand. When $S_T = 0$, reach zero line-voltage states by going to VII, because V contained two zero states in it. If $S_T = -1$, then regenerate, increasing the negative torque but decreasing the flux phasor; this is achieved by retarding the voltage phasor behind the flux phasor, but far away from it, and hence III is chosen. Note that it has two zeros in it, and, therefore, transition from VII to III requires a change of only one switch signal.

Implementation The drive scheme is realized as shown in Figure 8.12. Further, to reduce the voltage transducers, the information of line and phase voltages could be obtained from a single dc-link voltage transducer and the gate drive signals. Similarly, the phase currents can be reconstructed from a single dc-link current transducer and the gate drive signals of the inverter. In all, only two transducers are required, both of which are electrical; it does not require moving parts, thus making this control scheme robust and reliable. Further, the cost of the drive-system control is very low compared to that of position-sensor-based vector-controlled induction motor drives.

Performance The dynamic performance of this drive scheme is shown for both the torque- and the speed-controlled drive in Figures 8.13(a) and (b), respectively. The motor details are given in Example 5.4. The hysteresis windows for the torque and flux linkages are 0.05 p.u. and 0.001 p.u., respectively. The proportional and integral gains of the speed controller are 50 and 0.05, respectively. The base values of torque, speed, flux linkage, current, and voltage are 20.3 N·m, 377 rad/sec, 0.4213 Wb-turn,

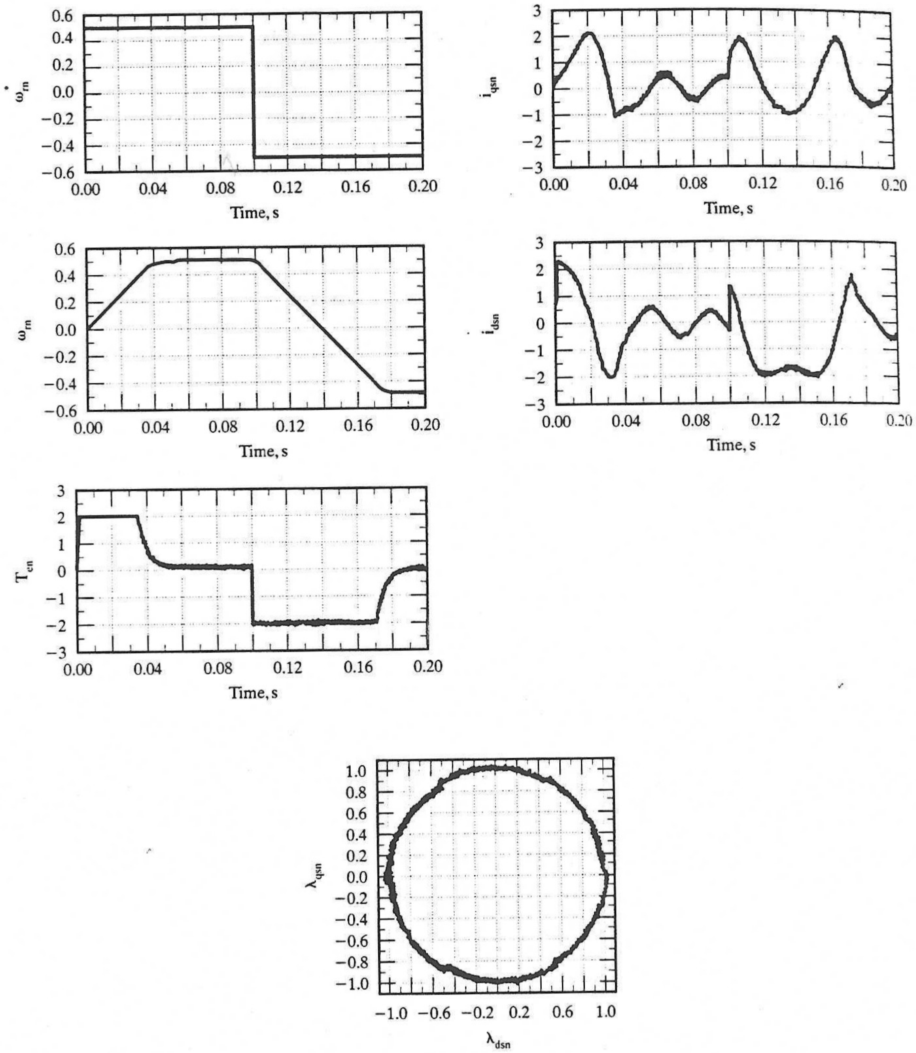

Figure 8.13(b) Dynamic performance of the speed-controlled drive system in normalized units

becomes uniform, as seen from its plot. The torque response is almost instantaneous, with considerable switching frequency ripples on it. The ripple torques have no effect on the speed, as shown from the speed-controlled drive.

The speed command is a step of 0.5 p.u. at starting and a step of 0.5 to −0.5 p.u. at 0.1 s. It is assumed that the machine has rated flux linkages at the time of application of the speed command. The electromagnetic torque is limited to ±2 p.u., which provides a faster acceleration, as is seen from the Figure 8.13(b). The rotor speed takes a smooth ramp profile with no oscillations, while the current is limited to two p.u. The locus of the stator flux-linkages phasor is almost a uniform circle, even during large speed changes and hence torque commands, thus showing the complete decoupling of the flux- from the torque-producing channels in the drive system.

$$i_{sn} = \sqrt{i_{dn}^2 + i_{qn}^2} = \sqrt{5.948^2 + 17.929^2} = 18.89 \text{ A} \quad (9.76)$$

$$i_{sk} = \sqrt{i_{dk}^2 + i_{qk}^2} = \sqrt{3.1679^2 + 25.34^2} = 25.537 \text{ A} \quad (9.77)$$

So even this narrow constant power speed range ratio $\omega_{max1} / \omega_b = 1.33$ is obtained at the price of higher stator current which implies lower power factor and, perhaps, efficiency. Reducing L_{sc} is a sure way to increase the value of ω_{max1} (9.71) and thus a wider constant power speed range is obtained. Leaving a voltage reserve at base speed or switching from a star to delta winding connection in the motor are two practical methods to widen the constant power zone.

9.9. IMPRESSING VOLTAGE AND CURRENTS THROUGH PWM

As already mentioned, for vector control, PWM is either closed-loop, that is a.c. current control driven (Figure 9.6), or open-loop, that is voltage waveform driven (Figure 9.10). PWM is thus a key part of vector control with voltage source inverters and has been given worldwide attention [15] with quite a few commercial implementation schemes.

9.9.1. Switching state voltage vectors

A PWM voltage source inverter (Figure 9.14) produces in the a.c. motor symmetrical rectangular voltage potentials V_{ap}, V_{bp}, V_{cp} provided that the conducting PES triplet is on for 60^0 electrical degrees. This means six pulses per period or six switchings per period only.

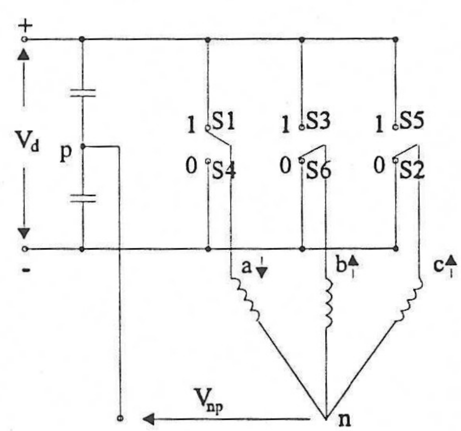

Figure 9.14. PWM voltage source inverter. One switch per leg conducting at any time

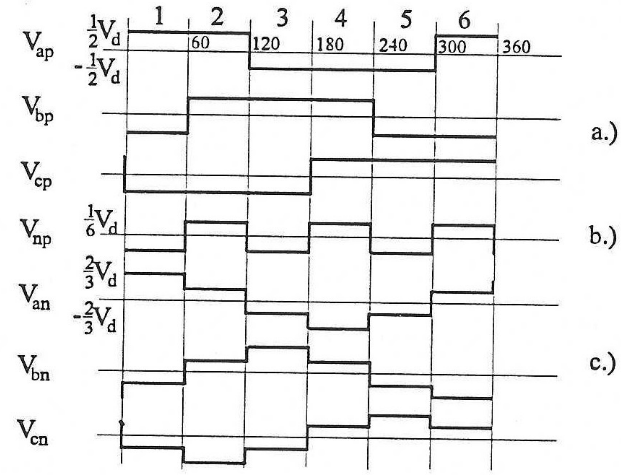

Figure 9.15. Voltage waveforms for six switchings per period
a.) Voltage potentials at motor terminals b.) neutral potential c.) phase voltages

The neutral potential V_{np} is either positive or negative as two upper or lower P.E.Ss in the inverter lag are on. V_{np} has three times the fundamental frequency and thus contains the triple harmonics which do not appear in the phase voltages V_{an}, V_{bn}, V_{cn}. This is true also when the conduction angle of various PES triplets is less than 60^0 via pulse width modulation (PWM) performed to modify the fundamental of the motor phase voltages.

The maximum voltage fundamental $V_{1six-step}$ is obtained for six-pulse switching and the modulation index m is

$$m = \frac{V_1}{V_{1six-step}}; \quad 0 \le m \le 1 \tag{9.78}$$

where from Figure 9.15a

$$V_{1six-step} = \frac{2}{\pi} V_0 \tag{9.79}$$

The ideal maximum modulation index is equal to unity. Various PWM schemes allow an $m_{max}<1$ which represents an important performance criterion as the inverter maximum kVA depends on the maximum voltage at motor terminals.

The PWM voltage source inverter allows for 6 SCR triplets that produce nonzero voltage space-vectors (Figure 9.14): (100, 110, 010, 011, 001, 101) and two zero voltage space-vectors (111, 000).

We may use space-phasors to describe the 6 nonzero switching situations as

$$\overline{V}_s(t) = \frac{2}{3}\left(V_{an}(t) + V_{bn}(t)\cdot e^{j\frac{2\pi}{3}} + V_{cn}(t)\cdot e^{-j\frac{2\pi}{3}}\right) \tag{9.80}$$

with V_{an}, V_{bn}, V_{cn} from Figure 9.15c, we obtain six space-phasors, 60^0 apart (Figure 9.16).

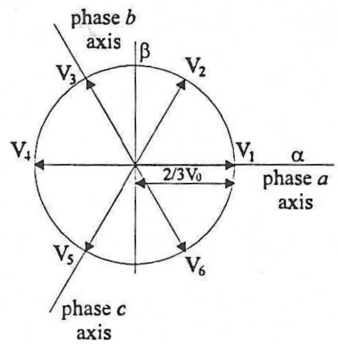

a.)

$\overline{V}_s$	V_1	V_2	V_3	V_4	V_5	V_6	V_0, V_7
	100	110	010	011	001	101	111, 000
V_{an}	$2/3V_0$	$1/3V_0$	$-1/3V_0$	$-2/3V_0$	$-1/3V_0$	$1/3V_0$	0
V_{bn}	$-1/3V_0$	$1/3V_0$	$2/3V_0$	$1/3V_0$	$-1/3V_0$	$-2/3V_0$	0
V_{cn}	$-1/3V_0$	$-2/3V_0$	$-1/3V_0$	$1/3V_0$	$2/3V_0$	$1/3V_0$	0

b.)

Figure 9.16. a.) Voltage space-vectors b.) The corresponding phase voltages

Timing the eight voltage space-vectors V_1, ..., V_8 is, in fact, the art of PWM. *Impressing the voltage commands* required by the vector control strategies may be done directly by *open-loop PWM. Impressing the current commands* through the same voltage space-vectors is done through *closed-loop PWM.* Among various PWM methods - treated extensively in the power electronics literature [15-16] - we deal with the two open-loop and two closed-loop PWM strategies considered here most representative.

9.9.2. Open-loop space-vector PWM

In space-vector PWM the reference voltage space-vector of the motor is treated directly and not phase by phase. The reference voltage space-vector V_1^* is sampled at a fixed clock frequency $2f_s$ (Figure 9.17a) being constructed through adequate timing of adjacent nonzero inverter voltage space-vectors V_1 to V_6 and the zero voltage space-vectors V_0, V_7 (Figure 9.17b)

$$2f_s(t_1V_i + t_2V_{i+1}) = V_s^*(t) \tag{9.81}$$

$$t_0 = \frac{1}{2f_s} - t_1 - t_2 \tag{9.82}$$

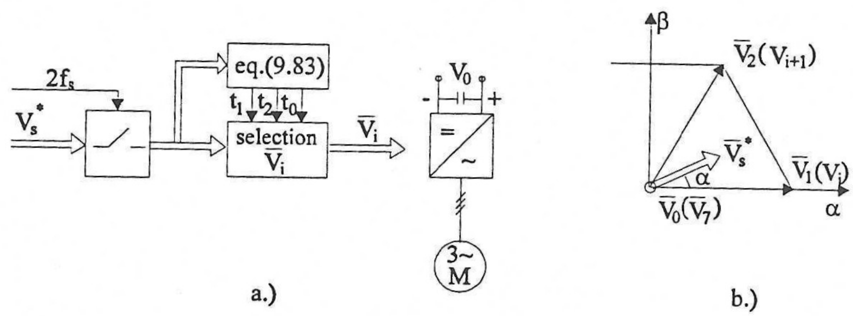

Figure 9.17. Open-loop space-vector PWM
a.) structural diagram b.) voltage space-vector in the first sector

The respective timings t_1, t_2 are

$$t_1 = \frac{1}{2f_s} V_s^*(t) \frac{2\sqrt{3}}{\pi} \sin\left(60^0 - \alpha\right) \tag{9.83}$$

$$t_2 = \frac{1}{2f_s} V_s^*(t) \frac{2\sqrt{3}}{\pi} \sin\alpha \tag{9.84}$$

In fact, this tehnique produces an average of three voltage space-vectors V_i, V_{i+1} and V_0 (V_7) over a subcycle $T = 1/2f_s$.

For the minimum number of commutations, with V_1^* in the first sector, the switching sequence is

$$V_0\left(t_0/2\right)\ldots V_1\left(t_1\right)\ldots V_2\left(t_2\right)\ldots V_7\left(t_0/2\right)\ldots \tag{9.85}$$

in all odd subcycles (of all 6 sectors) and

$$V_7\left(t_0/2\right)\ldots V_2\left(t_2\right)\ldots V_1\left(t_1\right)\ldots V_0\left(t_0/2\right) \tag{9.86}$$

for all even subcycles of all sectors.

Other sequences [17] might be imagined. For example,

$$V_0\left(t_0/3\right)\ldots V_1\left(t_1/3\right)\ldots V_2\left(t_2/3\right)\ldots V_2\left(t_2/3\right)\ldots V_1\left(t_1/3\right)\ldots V_0\left(t_0/3\right) \tag{9.87}$$

The loss factor is smaller in sequence (9.87) modified space-vector PWM than in ((9.85)-(9.86)).

The space-vector PWM produces high performance but requires prediction (online computation) of the reference voltage space-vector $V^*(t)$.

Carrier-based (or fixed frequency) PWM exhibits selected harmonics especially around the carrier frequency and thus produces increased noise in the machine. Distributing the harmonics energy over a large frequency band reduces noise. Random PWM does just that [18] - Figure 9.18.

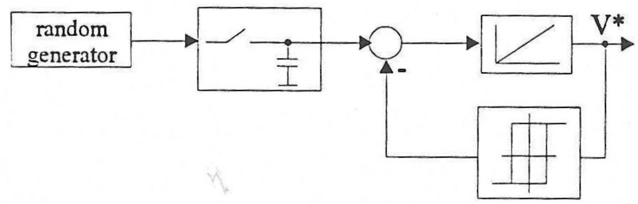

Figure 9.18. Random PWM principle

When the carrier signal reaches one of its peak values, its slope is reversed by a hysteresis block and a sample is taken from the random generator (Figure 9.18) which triggers an additional variation on the slope. This way the duration of subcycles is obtained while only the average switching frequency remains constant.

Overmodulation

The zero voltage timing decreases with the increase of reference voltage. This means that the reference voltage $\overline{V}_s^*$ touches the outer hexagon of the inverter space-vectors $\overline{V}_{1,...,6}$ (Figure 9.16b).

At this point the modulation index reaches $m_{max1} \approx 0.9$, and the next step would be six-pulse operation. Special overmodulation techniques are required for a smooth transition up to $m_{max2} = 1$ [15]. To further improve performance, optimized open-loop PWM methods have been introduced, especially for low switching frequency (GTOs) [15].

Dead time: effect and compensation

In order to prevent short-circuiting an inverter leg, there should be a lock-out time T_d between the turn-off of one PES and the turn-on of the next. T_d should be larger than the maximum particle storage time of the PES, T_{st}. The effect of the lock-out time T_d is a distortion ΔV on the reference voltage U^*.

$$V_{av} = V_s^* - \Delta V; \quad \Delta V = \frac{T_d - T_{st}}{T_d} \operatorname{sig}\bar{i}_s \tag{9.88}$$

The voltage distortion ΔV changes sign with current space-vector $\operatorname{sig}\bar{i}_s$ function

$$\operatorname{sig}\bar{i}_s = \frac{2}{3}\left[\operatorname{sign}(i_a) + e^{j\frac{2\pi}{3}}\operatorname{sign}(i_b) + e^{-j\frac{2\pi}{3}}\operatorname{sign}(i_c)\right] \tag{9.89}$$

and is proportional to safety time $T_d - T_{st}$.

This voltage distortion is considered by the fact that the on-time of the upper bridge arm is shortened by $T_d - T_{st}$ for positive current and is increased by the same amount for negative sign of current.